1 Introduction

Molecular self-assembly has given rise to a multitude of low periodic structures and therefore has attracted considerable interest in science and technology. Knowledge about self-assembly processes is indispensable for soft matter manipulation and the creation of novel nano-structured compounds. During the last decades, nano-technology became an integral part of many technical processes and products encountered in everyday life. It is considered as one of the key technologies [1] to cope with future tasks in health care and environmental protection.

In order to image and characterize matter at the nano-scale a multitude of techniques have been developed. Given the fact that conventional far field microscopy is diffraction limited, structures smaller than 200 nm can not be resolved. This restriction can be overcome by using probes with wavelengths which are shorter than visible light. Next to electrons which account for the resolving power of electron microscopes, X-rays and neutrons are employed to gain invaluable insight into the dynamics and composition of matter. In tomographic applications they penetrate the specimen, and magnified sectional images of the object can be created. X-ray diffraction allows to obtain structural information with a resolution better than 2 Å provided that the growth of highly purified crystals is possible.

Unfortunately, so far many substances have resisted all crystallization attempts or changed their physico-chemical properties as in the case of soft matter. Small angle X-ray scattering (SAXS) is complementary to X-ray diffraction and constitutes one of the most valuable techniques for a characterization of chemical assemblies like micelles, colloids, and gels. Furthermore, it does not require single crystals and allows probing heterogeneous solutions containing a structural ensemble.

In this thesis, SAXS has been utilized to pursue three different scientific questions which concern low-periodic structures ranging from microemulsions via proteinaceous hydrogels to β-barrel proteins.

1. Phase Transitions of Microemulsions to Liquid Crystals. Gels, liquid crystals and microemulsions are examples of thermodynamically stable nanostructures that evolve under suitable conditions (figure 1). Due to their chemical nature, microemulsions solubilize hydrophilic and hydrophobic compounds, a property which is crucial for the most diverse applications [2,3]. For instance, they are cheap and less toxic alternatives for organic solvents [4,5] and bear enormous potential as vehicles for transdermal drug delivery [6,7].

Microemulsions consisting of water, oil and surfactant systems have been investigated for a long time with respect to their complex behavior [8–10] and phase equilibria [11]. However, the phase transition processes themselves have not been covered and the kinetics remained elusive. Therefore, the question tackled is how phase transitions from microemulsions to liquid crystals occur and what are possible influence factors.

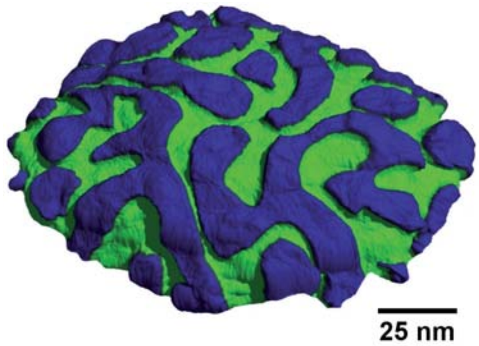

Figure 1: A microemulsion consists of interpenetrating oil and water domains. (Chapter 2 and 3.)

For this reason, the nature of these self-assembly processes has been investigated as a function of concentration and alkyl chain length of the surfactant molecules. Doping of the mixture with dye molecules allowed to photo-induce the transformation and to probe the structural changes by SAXS experiments.

It will be demonstrated that the surfactant concentration has a direct impact on the length of the induction time, i.e. the amount of time that passes until onset of the transformation. This finding is related to the morphology of the microemulsion and can be explained by a dispersion of the activation energy.

2. Hydrogel Formation of the Nucleoporin Nsp1p. Gels are nanostructures consisting of a three-dimensional macromolecular meshwork in which a solvent is homogenously dispersed. Crosslinking of (bio)-polymer chains by dipolar, ionic or covalent interactions confers stability to the material and allows to create complex internal structures [12] with controllable physical properties. This opens the door for a wide range of applications in the production of stable nanoparticles [13, 14] and in the field of biotechnology [15–17]. Embedding enzymes and their co-factors [18–20] in gels retains their biological functionality and allows their utilization as easily recoverable biocatalysts.

Proteinaceous gels from the yeast nucleoporin Nsp1 are of particular interest in biology because of their outstanding selectivity properties. Small objects are allowed to enter freely, whereas the transit of macromolecules which exceed a critical size is efficiently suppressed. This feature makes them an ideal model system for transport processes into the cellular nucleus in particular but also for the development of highly selective nano-materials in general.

Recently, Ader et al. [21] found evidence for the existence of β-sheet elements in nucleoporin hydrogels and proposed a hydrophobic collapse to occur during gelation. Given many outstanding scientific questions, the aim of this thesis is to clarify the sol-gel process and to reveal the structural characteristics that might be crucial for their selectivity properties. Consequently, time-resolved optical spectroscopy and X-ray scattering experiments have been performed in order to study the sol-gel transition and to reveal the emergence of hydrophobic interactions. One key aspect is the reconstruction of three-dimensional models representing integral building blocks of the hydrogel and the quantitative determination of the β-sheet content. Moreover, the investigations address the average mesh sizes as well as inter β-strand and β-sheet distances. In total, the structural hierarchy of the network which is determined by the balance of attractive and repulsive interactions will be characterized in detail.

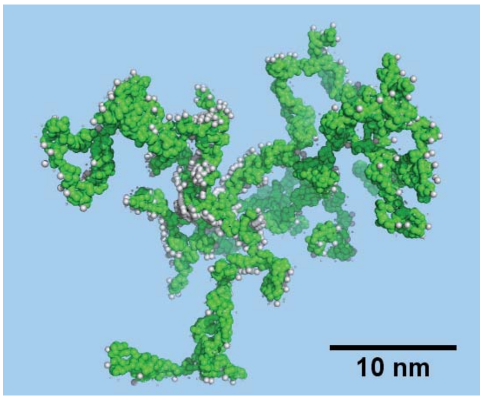

Figure 2: The three dimensional model shows characteristic elements of the Nsp$1^{2\text{-}601}$ hydrogel. (Chapter 5.)

3. β-barrel Dynamics of Dronpa during Photoswitching. β-barrel proteins represent one class of proteins with low periodic structures, in which β-sheets are a prominent structural motif. For instance, in the green fluorescent protein (GFP) [22] the β-sheets are folded in an 11 stranded β-barrel wrapped around a single α-helix which holds the autocatalytically formed chromophore. The β-barrel topology serves to protect the chromophore from external fluorescence quenchers and accounts for the mechanical stability of the protein [23, 24].

Dronpa is a variant of GFP and can be reversibly photoswitched from a fluorescent bright state [25] to a non-fluorescent dark state [26]. In this regard, it is the paradigm of the class of reversibly photoswitchable proteins and has stimulated the generation of new variants which differ in switching speeds or colors [27, 28]. Due to its remarkable switching characteristics, it is of enormous interest for live cell imaging [29], fluorescence microscopy [30–32], protein tracking [33] and more strikingly also for data storage [34].

Despite considerable knowledge from X-ray crystallography about the static structure of Dronpa in its fluorescent bright (figure 3) and photoswitched dark state, conformational changes occurring during photoswitching could not be observed so far. The question arises, does photoswitching lead to dynamic changes of the β-barrel topology?

This is of utmost importance for the development of future variants. For this aim time-resolved SAXS experiments exploiting the high brilliance of third generation synchrotron sources have been performed (chapter 6). These data will unveil the structural dynamics in terms of slow correlated motions upon optical excitation. It will be shown that photoswitching is not locally restricted to the chromophore but has an impact on the overall β-barrel topology.

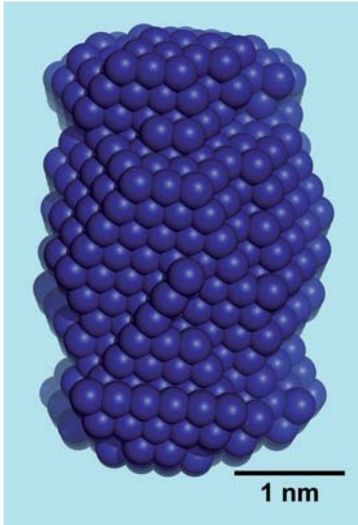

Figure 3: β-barrel shape of Dronpa in solution obtained by small angle X-ray scattering. (Chapter 6.)

Outline. The following paragraph delineates the organization of this thesis. Chapter 2 gives an overview of microemulsions and liquid crystals and covers their phase transition kinetics as a function of the surfactant concentration. The scope of this investigation is extended in chapter 3 which concentrates on the alkyl chain length of the involved reagents. Chapter 4 gives an introduction on solution X-ray scattering as a tool to study proteins which is of relevance for the following chapters. Chapter 5 casts light on the formation and structural characterization of an FG hydrogel derived from the yeast nucleoporin Nsp1p. The sixth chapter is devoted to the structural dynamics of the reversibly photoswitchable protein Dronpa upon optical excitation of the chromophore. At the end of this work a résumé of this thesis and documentation of multiple LABVIEW programs [35] can be found.

It should be noted that there is no chapter about the theoretical background of these experiments since necessary fundamental principles and the development of time resolved X-ray scattering methods are presented within the experimental parts.

2 Photoinduced Phase Transition from Microemulsions to Liquid Crystals: Effect of Surfactant Concentration

2.1 Introduction

In this section, phase transitions from the microemulsion phase to the liquid crystal phase in a mixture of non-ionic surfactants are studied. Poly-alkyl glycol ethers are non-ionic surfactants which solubilize effectively hydrophobic as well as hydrophilic reagents due to their amphiphilic character (figure 4). They exhibit various thermodynamically stable phases with low periodic order on the nanometer to micrometer length scale.

Depending on the temperature and concentration, a wide range of structures evolve including spherical or cylindrical micelles, lamellar phases and bicontinuous structures [36]. The most prominent phases formed from a ternary mixture of a polar solvent, a nonpolar solvent and an amphiphilic agent are microemulsions (ME) or liquid crystals (LC). These phases are related by the different arrangement of the polar and apolar regions in space and have been studied with emphasis on their structure and stability [37]. In addition to their potential for drug delivery [6], microemulsions serve as model systems for studying a range of fundamental liquid state phenomena,

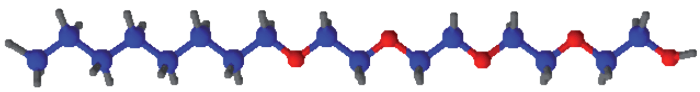

(a) C_8E_4

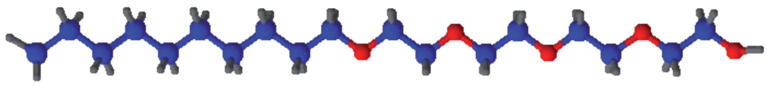

(b) $C_{10}E_4$

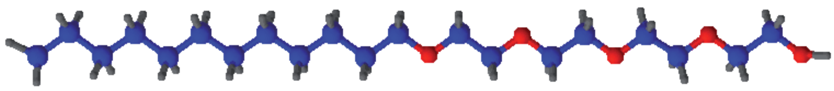

(c) $C_{12}E_4$

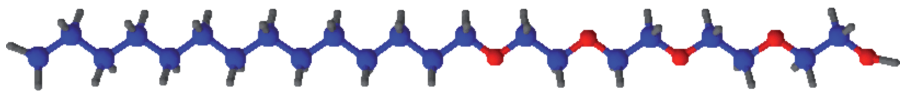

(d) $C_{14}E_4$

Figure 4: Chemical structure of the non-ionic surfactants. a) tetraethylene glycol monooctyl ether (C_8E_4), b) tetraethtylene glycol monodecyl ether ($C_{10}E_4$), c) tetraethylene glycol monododecyl ether ($C_{12}E_4$) and d) tetraethylene glycol monotetradecyl ether ($C_{14}E_4$).

e. g. calculation of the oil-water interfacial free energy, nucleation, Ostwald ripening, solubilization kinetics, the Hofmeister effect and vesicle fusion [38].

Especially at the phase boundary to liquid crystals, large concentration fluctuations appear which determine the dynamic properties of the system. Self-assembly processes of solvated molecules like lipids, proteins and synthetic polymers which occur at this interface are characterized by many poorly understood ordering phenomena [39]. For this reason, it is an important task and great challenge to develop effective and environmentally benign methods, which allow to rationalize and control phase transitions [40].

In principle, self-assembly processes can either be temperature or laser-induced. Laser-induced self-assembly has been employed for amphiphilic molecules at the gas-liquid interface [41], at the liquid-solid interface [42] and at the liquid-liquid interface [43]. Light irradiation provides means to align molecules and to induce phase changes via the absorption of optical photons. Excitation of photo-reactive compounds leads to a warming of the sample and causes chemical reactions whose products are predicted by the Woodward-Hoffmann [44] rules. However, the optical activity of the system under investigation limits these methods to certain special cases.

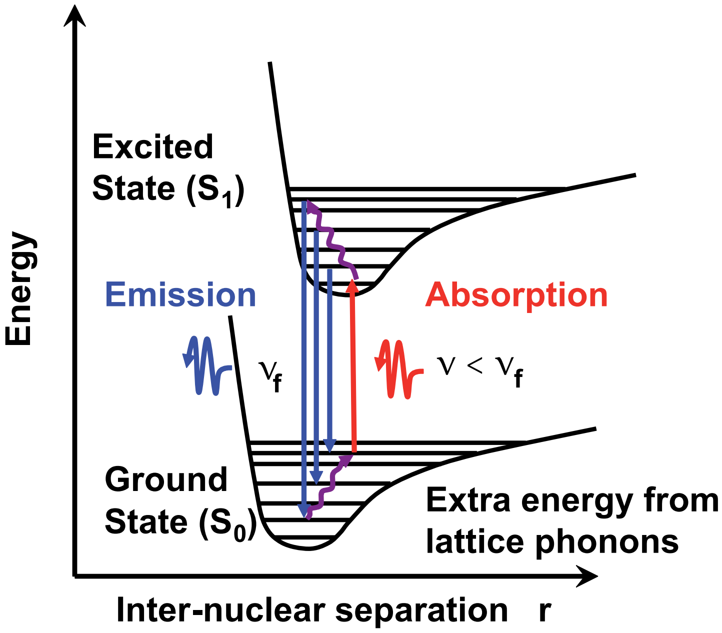

Figure 5: Principle of laser cooling. Absorption of optical photons leads to an excitation from a vibrational "hot" state of the electronic ground state to the first excited state from which fluorescence is possible. The energy gain is due to collisions and lattice phonons. Extraction of energy from the system then occurs by fluorescence.

Photo sensitization realized by the addition of dyes like Rhodamine 101 extends the possibility to photo induce phase transitions to any arbitrarily chosen matter, which otherwise are inherently inert against optical excitation. Anti-Stokes excitation of a dye [45, 46] by continuous laser irradiation with 632.8 nm can be employed to extract energy from the system (figure 6b).[1]

[1]The temperature of liquids ($V = 0.3\,\mathrm{ml}$, $c = 1 \cdot 10^{-4}\,\mathrm{mol/l}$ Rhodamine 101, $P_{laser} = 350\,\mathrm{mW}$) could be effectively reduced by 3 K in a period of 4 h [45].

This is done by exciting dye molecules (figure 6a) from vibrational "hot" states of the electronic ground state (S_0) to the lowest vibrational level ($\nu = 0$) of the first excited state (S_1). Intramolecular vibrational energy redistribution processes then lead to the emission of photons which are higher in energy than the absorbed ones. Hence, the emitted photons reduce the overall energy of the solution (figure 5). In total, this sequence of events can be regarded as an example of one-photon frequency up-conversion processes. Considering the high fluorescence quantum yield of Rhodamine 101 ($\Phi = 1.00$ [47]), it becomes clear that other deactivation pathways like internal conversion or excimer formation can be neglected.

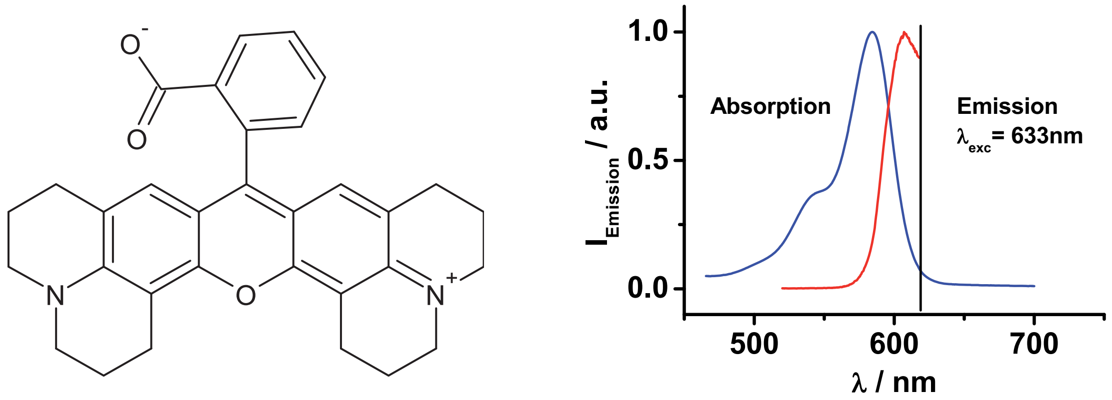

(a) Rhodamine 101 **(b)** Optical properties

Figure 6: a) Chemical structure of the laser-dye Rhodamine 101. b) Absorption and fluorescence emission spectra of Rhodamine 101 solvated in liquid crystals formed from $C_{10}E_4$, water, decane and cyclohexane.

Energy redistribution processes by means of collision and diffusion then result in an overall decrease of temperature within the whole sample volume. The rate is limited by the ratio of incoming optical photons and the number of photo-excitable dye molecules.

In this study, the concept of Anti-Stokes excitation has been applied for the first time to investigate the phase transition from the microemulsion to the liquid crystal phase as a function of surfactant concentration.

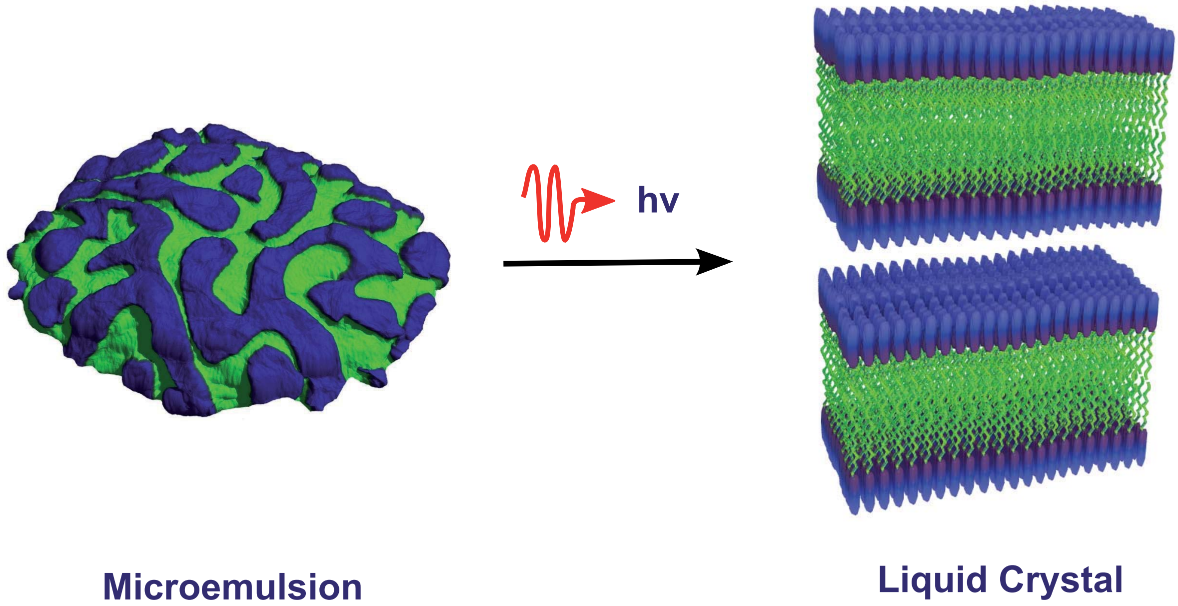

Figure 7: Illumination of a dye doped microemulsion with red light ($\lambda = 632.8\,\mathrm{nm}$, $P = 3\,\mathrm{mW}$) induces a phase transition to the liquid crystalline phase. Blue and green denote hydrophilic and hydrophobic regions of the microemulsion and liquid crystal, respectively.

The microemulsion chosen as a model system consists of $C_{10}E_4$, water, n-decane and cyclohexane. Variation of the surfactant mass fraction (γ) at equal volume fractions of water and oil leads to the phase diagram depicted in figure 8.

In the two-phase region, the mixture is divided macroscopically into an aqueous and oil-rich phase. Depending on the temperature, the amphiphilic molecules feature a higher affinity for one or the other phase. In the microemulsion phase, the amphiphilic solutions appear macroscopically as one phase. In reality, the phase is separated on the microscopic scale with the oil and water domains held in contact by the surfactant molecules [9]. Therefore, it can be visualized as a collection of droplets with water and oil domains of colloidal size which are separated by a layer of surfactant with either micelle or inverse micelle structure.

At concentrations where the microemulsion contains equal volumes of water and oil, a bicontinuous microemulsion is formed (figure 7). It consists of interpenetrating domains with equal length scales [48] and short range order [49]. The properties of bicontinuous microemulsions depend to a large

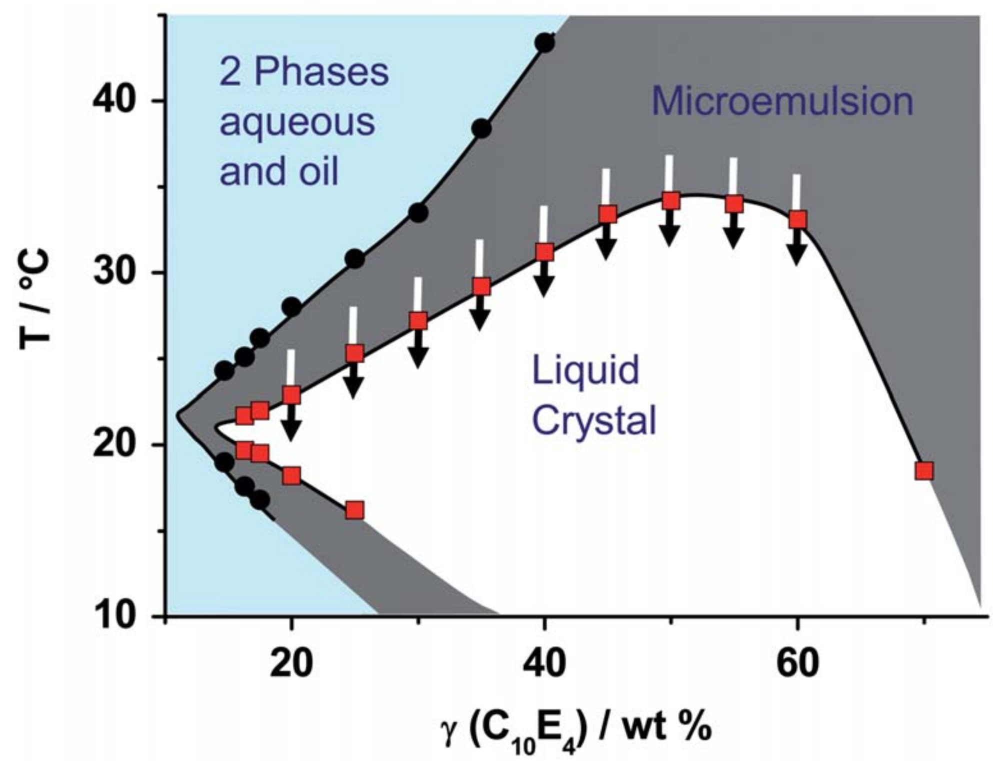

Figure 8: Phase diagram of the system $C_{10}E_4$, water, *n*-decane and cyclohexane at equal volume fractions of water and oil. Cyan represents an area where two phases coexist, dark grey is the microemulsion phase and white the liquid crystal phase. The dots represent points of the phase boundaries as measured by the polarized screening technique. Arrows indicate the concentrations at which the microemulsion to liquid crystal phase transition has been photo-induced.

extent on the bending moduli of the surfactant containing oil-water interface and can be altered through the addition of copolymers [50] and alcohols [51].

At intermediate temperatures the formation of lyotropic liquid crystals with a long range lamellar order (figure 7) and anisotropic behavior of hydration is favored [52]. Liquid crystalline phases are classified according to their orientational order as nematic or smectic assemblies but also depending on their formation modes. Thermotropic liquid crystals are formed as a consequence of temperature changes whereas lyotropic liquid crystals emerge due to variations in concentration.

In this study, the LC phase is a thermotropic smectic assembly with interlamellar spacings ranging from $d = 80$ Å to $d = 130$ Å. The magnitude of these lattice parameters can ideally be investigated by X-ray scattering techniques. Interestingly, the macroscopic appearance of the liquid crystal formed by laser cooling exhibits a unique texture ("oily streaks") over the whole volume of the capillary which is quite different from the one formed after temperature reduction. Therefore, it is concluded that interaction of the laser field through the induced dipole moment of the molecules generates a molecular alignment which finally causes a preferred orientation of the crystallites. A temperature induced phase transition, in contrast, leads to the creation of isotropically distributed liquid crystalline domains. Figure 9a shows a characteristic micrograph of such a dye-doped microemulsion at the initial state. The differences of a liquid crystal phase created via photo induction and temperature induction are well visible through a microscope with crossed polarizers. The former (figure9b) displays long stripes along the direction of the capillary whereas the latter (figure 9c) shows a mosaic-like pattern due to a random arrangement of the liquid crystalline domains. All the photographs were taken 20 hours after induction of the phase transition. Based on the experiments performed, the temperature decrease achieved by Anti-Stokes excitation has been determined in the range of 1 K to 2 K. In the following the nature and mechanism of these self-assembly processes which lead to such pattern formation in the LC phases will be studied by time-resolved X-ray scattering (figure 11).

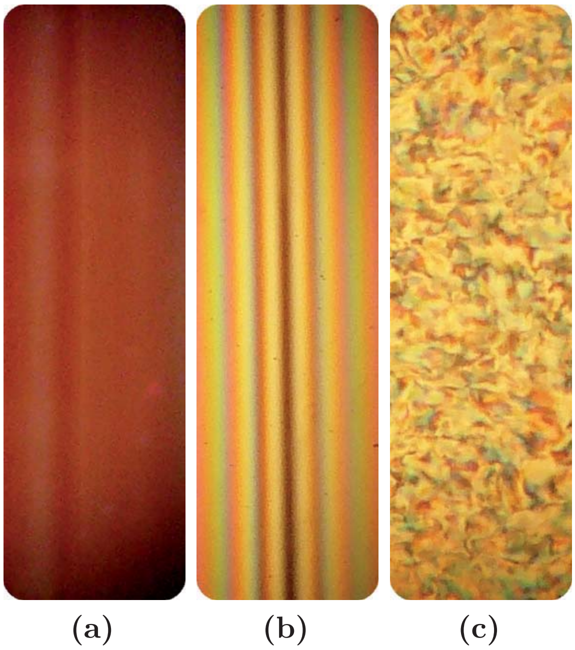

Figure 9: a) Micrograph of the initial dye-doped microemulsion. b) Polarized light micrographs of the lamellar phase after photo induction. c) Polarized light micrographs of the lamellar phase after temperature-induced phase transitions.